



COVID-19 Research Tools

Defeat the SARS-CoV-2 Variants

InvivoGen



Albumin-Based Drug Delivery as Novel Therapeutic Approach for Rheumatoid Arthritis

This information is current as of August 9, 2022.

Andreas Wunder, Ulf Müller-Ladner, Ernst H. K. Stelzer, Jürgen Funk, Elena Neumann, Gerd Stehle, Thomas Pap, Hannsjörg Sinn, Steffen Gay and Christoph Fiehn

J Immunol 2003; 170:4793-4801; ;
doi: 10.4049/jimmunol.170.9.4793
<http://www.jimmunol.org/content/170/9/4793>

References This article **cites 38 articles**, 6 of which you can access for free at:
<http://www.jimmunol.org/content/170/9/4793.full#ref-list-1>

Why *The JI*? [Submit online.](#)

- **Rapid Reviews! 30 days*** from submission to initial decision
- **No Triage!** Every submission reviewed by practicing scientists
- **Fast Publication!** 4 weeks from acceptance to publication

**average*

Subscription Information about subscribing to *The Journal of Immunology* is online at:
<http://jimmunol.org/subscription>

Permissions Submit copyright permission requests at:
<http://www.aai.org/About/Publications/JI/copyright.html>

Email Alerts Receive free email-alerts when new articles cite this article. Sign up at:
<http://jimmunol.org/alerts>

The Journal of Immunology is published twice each month by
The American Association of Immunologists, Inc.,
1451 Rockville Pike, Suite 650, Rockville, MD 20852
Copyright © 2003 by The American Association of
Immunologists All rights reserved.
Print ISSN: 0022-1767 Online ISSN: 1550-6606.



Albumin-Based Drug Delivery as Novel Therapeutic Approach for Rheumatoid Arthritis¹

Andreas Wunder,* Ulf Müller-Ladner,^{2†} Ernst H. K. Stelzer,[‡] Jürgen Funk,[§] Elena Neumann,[†] Gerd Stehle,[¶] Thomas Pap,^{||} Hannsjörg Sinn,* Steffen Gay,^{||} and Christoph Fiehn[§]

We reported recently that albumin is a suitable drug carrier for targeted delivery of methotrexate (MTX) to tumors. Due to pathophysiological conditions in neoplastic tissue, high amounts of albumin accumulate in tumors and are metabolized by malignant cells. MTX, covalently coupled to human serum albumin (MTX-HSA) for cancer treatment, is currently being evaluated in phase II clinical trials. Because synovium of patients with rheumatoid arthritis (RA) shares various features observed also in tumors, albumin-based drug targeting of inflamed joints might be an attractive therapeutic approach. Therefore, the pharmacokinetics of albumin and MTX in a mouse model of arthritis was examined. Additionally, uptake of albumin by synovial fibroblasts of RA patients and the efficacy of MTX and MTX-HSA in arthritic mice were studied. The results show that when compared with MTX, significantly higher amounts of albumin accumulate in inflamed paws, and significantly lower amounts of albumin are found in the liver and the kidneys. The protein is metabolized by human synovial fibroblasts *in vitro* and *in vivo*. MTX-HSA was significantly more effective in suppression of the onset of arthritis in mice than was MTX. In conclusion, albumin appears to be a suitable drug carrier in RA, most likely due to effects on synovial fibroblasts, which might increase therapeutic efficacy and reduce side effects of MTX. *The Journal of Immunology*, 2003, 170: 4793–4801.

In rheumatoid arthritis (RA),³ the synovial lining layer of affected joints is transformed into a highly proliferative so-called pannus-like tissue consisting of synovial fibroblasts (SFs), synovial macrophages, and various infiltrating inflammatory cells. This hypertrophic and edematous tissue progressively invades adjacent cartilage and bone (1–3). Subsequently, joint destruction is mediated by matrix-degrading enzymes released specially by transformed-appearing activated SFs. Similar phenomena are also observed in neoplastic diseases (4, 5). Because of the increased rate of cell division in RA and cancer, both diseases are treated with antiproliferative drugs like methotrexate (MTX), which is probably the most common drug in RA treatment (6, 7) and is also part of numerous treatment protocols in oncology (8, 9).

Unfortunately, progression of joint destruction in most RA patients cannot be completely inhibited by MTX treatment. Large

amounts of the administered MTX are eliminated by the kidneys within a short period of time, resulting in short plasma half-life and low drug concentration in the target tissue. Increased doses often result in a higher therapeutic efficacy, but a higher risk of side effects as well, limiting the dose that can be administered (6, 7). Thus, the disadvantageous pharmacokinetic properties of MTX are probably the basis of unsatisfactory treatment results (10–12).

To overcome the lack of specificity with regard to the target tissue, drugs can be covalently coupled to suitable drug carriers. Main features of appropriate drug carriers are high accumulation in the target tissue, low uptake rates in normal tissue, low toxicity, the biochemical potential to be linked to drugs, and release of the drug in the target tissue, as well as the general availability and affordability (13, 14). The plasma protein albumin fulfills these requirements for delivery of drugs into tumors as demonstrated by a number of studies.

Primary investigations have shown that tumors metabolize substantial amounts of albumin, using it as source for nitrogen and energy (15), and that tumors metabolize plasma proteins more efficiently than free amino acids (16). Several studies with tumor-bearing animals have provided further evidence that albumin accumulates in tumors because of their altered physiology and metabolism (17–19). Due to the leakiness of tumor vessels, the rate of albumin extravasation is markedly increased. Moreover, the lack of a functional lymphatic system results in the accumulation of albumin in the tumor tissue (20). The uptake of albumin in tumor cells itself occurs by fluid phase endocytosis followed by lysosomal breakdown. As a result, albumin-coupled drugs are liberated within the tumor cells (17–19).

Due to the high rate of accumulation and metabolism in tumor tissue compared with normal tissue, its stability, and the large number of different binding sites, numerous efforts have been made to use albumin as drug carrier for MTX. All of these attempts have failed, because albumin was denatured either by the coupling procedure or by the conjugation of up to 50 molecules of MTX covalently coupled to one molecule of albumin. This resulted in

*Department of Radiochemistry and Radiopharmacology, German Cancer Research Center, Heidelberg, Germany; [†]Division of Rheumatology and Clinical Immunology, Department of Internal Medicine I, University of Regensburg, Germany; [‡]Cell Biophysics/Cell Biology Program, European Molecular Biology Laboratory, Heidelberg, Germany; [§]Department of Hematology, Oncology and Rheumatology, Clinic of Internal Medicine V, and [¶]First Department of Medicine, Faculty of Clinical Medicine, Mannheim, University of Heidelberg, Heidelberg, Germany; and ^{||}World Health Organization Collaborating Center for Molecular Biology and Novel Therapeutic Strategies for Rheumatic Diseases, University of Zurich, Zurich, Switzerland

Received for publication September 3, 2002. Accepted for publication February 18, 2003.

The costs of publication of this article were defrayed in part by the payment of page charges. This article must therefore be hereby marked *advertisement* in accordance with 18 U.S.C. Section 1734 solely to indicate this fact.

¹ This work was supported by the Medical Faculty of the University of Heidelberg (Grant 354/2000 to C.F. and A.W.) and by the Deutsche Forschungsgemeinschaft (Grant Mu 1383/3-3 to U.M.-L.).

² Address correspondence and reprint requests to Dr. Ulf Müller-Ladner, Department of Internal Medicine I, University of Regensburg, D-93042 Regensburg, Germany. E-mail address: ulf.mueller-ladner@klinik.uni-r.de

³ Abbreviations used in this paper: RA, rheumatoid arthritis; SF, synovial fibroblast; MTX, methotrexate; HSA, human serum albumin; CIA, collagen-induced arthritis; CLSM, confocal laser scanning microscopy; DTPA, diethylenetriaminopentaacetic acid; AFLe, aminofluorescein; MTD, maximum tolerated dose; SLE, systemic lupus erythematosus.

high immunogenicity and in a considerable uptake of the conjugates by the reticuloendothelial system. Subsequently, these conjugates were removed rapidly from the circulation and were taken up in large amounts by the liver, resulting in low concentrations in the tumor (21, 22).

We have previously reported a new conjugate of MTX coupled covalently to human serum albumin (MTX-HSA) to improve the unfavorable pharmacokinetic properties of MTX for cancer treatment. Using the coupling procedure developed in our laboratory and exerting a 1:1 molar loading ratio, the distribution pattern of the conjugate *in vivo* is identical with underivatized albumin, demonstrating that the native character of the protein is not affected (21, 22). Preclinical studies have shown antitumor activity of MTX-HSA in rat tumor models (23, 24) and in a variety of human xenograft tumors in nude mice (25). Furthermore, MTX-HSA has shown promising results on the tumor growth, a plasma half-life equivalent to that of HSA, and no immunogenicity, and it was well tolerated in a clinical phase I trial for cancer treatment (26). At present, the conjugate is under clinical investigation in phase II clinical trials.

Several publications led to the idea that albumin might also be a suitable drug carrier to target drugs to inflamed joints of patients with RA (1–5, 27–30). Therefore, albumin-based drug conjugates like MTX-HSA could be an attractive novel therapeutic approach. The permeability of the blood-joint barrier for albumin in inflamed joints of RA patients is markedly increased (27). Moreover, patients with active RA, as well as cachectic cancer patients (19), frequently develop hypoalbuminemia due to increased albumin turnover, presumably caused by high albumin consumption at sites of inflammation (28–30). Similar to tumor cells, metabolism of synovial cells is highly up-regulated, showing an active metabolic state accompanied by a high demand for nitrogen and energy (1–5). Thus, accumulation of albumin in inflamed joints due to increased extravasation, uptake, and metabolism of albumin in proliferating synovial cells with high protein turnover seems likely.

In the absence of data addressing the absolute amount of albumin uptake and its kinetics in inflamed joints and metabolism in synovial cells, we performed studies to investigate the pharmacokinetics of radiolabeled albumin compared with radiolabeled MTX in mice with collagen-induced arthritis (CIA). To visualize albumin uptake by arthritic paws, scintigraphy and laseroptical experiments using fluorescence-labeled albumin were performed. To investigate albumin uptake by SFs from patients with RA as possible target cells of albumin-coupled drugs *in vivo*, the cells were implanted together with healthy human articular cartilage to SCID mice and were examined histologically by fluorescence microscopy after application of fluorescence-labeled albumin. Metabolism of albumin in SFs from RA was studied by confocal laser-scanning microscopy (CLSM) *in vitro* using fluorescence-labeled albumin. Finally, the effects of MTX-HSA and MTX on the development of arthritis in mice were evaluated.

Materials and Methods

Reagents

HSA was purchased from Pharma Dessau (Dessau, Germany). Diethylenetriaminepentaacetic acid (DTPA), DMSO, *N,N'*-dicyclohexylcarbodiimide, *N*-hydroxysuccinimide, and 1,2,4-trihydroxyanthracinone (purpurin) were provided by Aldrich (Steinheim, Germany). ^{111}In was obtained from NEN Life Science (Zaventem, Belgium). For separation of the compounds, ultrafiltration units (exclusion size 30 kDa) from Millipore (Eschborn, Germany) were used. Aminofluorescein (AFLc), bovine type II collagen, acridine orange, and MTX were purchased from Sigma-Aldrich (Deisenhofen, Germany). Tritium-labeled MTX (3',5',7'-[^3H](*N*)-MTX) was obtained from Moravik Biochemicals (Brea, CA). IFA and *Mycobacterium tuberculosis* H 37 RA were purchased from Difco/BD Biosciences (Detroit, MI).

Tissue Solubilizer BTS 450 and Ready Protein Scintillation Cocktail were provided by Beckman Instruments (Irvine, CA). All products for cell culture were bought from Life Technologies (Eggenstein, Germany).

Preparation of radiolabeled HSA (^{111}In -DTPA-HSA)

Radioactive-labeled albumin was prepared as previously described (18). In brief, DTPA was coupled covalently to HSA at a molar ratio of 1:1. For radiolabeling, $^{111}\text{InCl}_3$, dissolved in hydrochloric acid, was mixed with sodium citrate to form indium citrate complexes. This mixture was added to DTPA-HSA. Finally, the low-m.w. compounds were removed from ^{111}In -DTPA-HSA by ultrafiltration. The labeling yield was ~97%, with protein. Analytical HPLC control runs of the tracer showed no intermolecular cross-linking of purified ^{111}In -DTPA-HSA. The HPLC profile of radiolabeled HSA was consistent with the profile of unmodified HSA.

Fluorescence labeling of HSA with AFLc (AFLc-HSA) and purpurin (purpurin-HSA)

For the covalent coupling of AFLc to albumin in a 1:1 molar ratio, 4 g of HSA (diluted in 20 ml of saline), 20 ml of 0.17 M NaHCO_3 , and 15 ml of methanol were combined. With continuous stirring, 45 mg of AFLc, diluted in 4 ml of DMSO, was added. After 1 h, 350 ml of H_2O was added, and the low-m.w. compounds were separated by ultrafiltration. This step was repeated five times. Finally, the purified AFLc-HSA conjugate was diluted in sodium bicarbonate buffer (0.17 M, pH 8.4), and the concentration of AFLc was determined by absorbance at 497 nm. Quality controls were conducted by HPLC analysis. No polymer formation was observed during the conjugation procedure. The HPLC profile of AFLc-HSA was consistent with the profile of HSA. The covalent coupling of purpurin to albumin is described in a pending patent (DP19847362.1).

Coupling of MTX to HSA (MTX-HSA)

MTX-HSA was prepared as described previously, using *N,N'*-dicyclohexylcarbodiimide and *N*-hydroxysuccinimide for activation and linking MTX to HSA (21).

Cell culture of SFs

Synovial tissue was obtained from a patient with RA undergoing joint replacement surgery. The synovial membrane was dissected, and SFs were isolated as described previously (31). The cells were cultured in DMEM, supplemented with 10% heat-inactivated FCS and penicillin-streptomycin, and characterized as SFs by morphologic and immunocytochemical criteria.

Animals and arthritis models

All animal experiments were approved by the German Federal Government. A total of 283 male DBA-1 mice, 7–8 wk of age, were obtained from M&B (Ry, Denmark). The mice were maintained in the central animal house at the University of Heidelberg (Germany). CIA was induced according to the procedure described by Wooley (32). Bovine type II collagen was dissolved in 0.1 M acetic acid at a concentration of 2 mg/ml by stirring for ~3 h at 4°C. To prepare the adjuvant, 3 mg of heat-inactivated *M. tuberculosis* was added to 1 ml of IFA. Equal volumes of the collagen solution and the adjuvant were emulsified at 4°C. The mice were immunized by three intradermal injections of the emulsion at the base of the tail (50 μl each). Three weeks after the first immunization, the procedure was repeated. Within 2 wk after the second immunization, ~70% of the mice developed arthritis characterized by erythema and swelling of the paws. In the majority of mice, the disease progressed to two or more paws.

To examine albumin uptake by SFs *in vivo*, 18 female Crl-scidBR 4-wk-old SCID mice were obtained from a germ-free breeding colony (Charles River Breeding Laboratories, Sulzfeld, Germany) and were housed under Institutional Animal Care and Use Committee-approved germ-free conditions at the University of Regensburg (Germany). The animals were examined for macroscopic anomalies before and during surgery as well as for macro and histopathologic abnormalities after sacrifice. At the day of implantation, normal human cartilage was obtained from nonarthritic knee joints of patients undergoing routine surgery at the Department of Orthopedics at the University of Regensburg. Implantation of fibroblasts and cartilage was performed under sterile conditions using the novel "inverse wrap" technique (33). A cube-like piece of inert sponge (80–100 mm 2) was incised and a piece of cartilage (3–5 mm 2) was inserted into its center. The sponge was then soaked in fibroblasts (5 \times 10 5 cells) suspended in sterile saline. The skin of the anesthetized mouse was opened surgically, and two pieces of sponge containing cartilage and fibroblasts were inserted.

Laseroptical experiments

To visualize albumin uptake in paws affected by arthritis, 10 DBA-1 mice with CIA were distributed randomly between two groups. Forty micrograms of free AFLc (control) and 40 μg of AFLc covalently coupled to albumin (AFLc-HSA), dissolved in 40 μl of sodium bicarbonate buffer (0.17 M, pH 8.4), were administered to five mice each by i.v. injection into a lateral tail vein. After 3 h, the mice were anesthetized and their paws were illuminated using an argon laser (Spectra Physics, Mountain View, CA) at a wavelength of 488 nm. Fluorescence from illuminated paws was detected using a long-pass barrier filter of 520 nm. Fluorescence and white light images were taken with a conventional camera using color slide film.

Pharmacokinetics of radiolabeled albumin and sequential scintigraphy

To quantify circulation times and uptake of albumin in healthy and inflamed paws, as well as in the liver and kidneys at different time points, 35 mice with CIA and 21 healthy control mice, distributed randomly among seven groups, received an i.v. injection of ~ 7.4 MBq of radiolabeled HSA (^{111}In -DTPA-HSA), dissolved in 50 μl of sodium bicarbonate buffer (0.17 M, pH 8.4). To study the distribution of the tracer substance by scintigraphy, the animals were placed on a multihole collimator (420 keV) of a 10-inch gamma camera (Pho-Gamma IV; Searle-Siemens, Erlangen, Germany). For online evaluation of the data, a computer system specially adapted to the gamma camera was used (Gaede Medworker; Gaede, Freiburg, Germany). Static images (5 min each) were registered 10 min and 1, 3, 8, 13, 24, and 48 h after tracer injection. Five mice with CIA and three control mice without arthritis were sacrificed at each point of the time course. All paws, liver, and kidneys were prepared and weighed, and blood samples were drawn. Radioactivity in the blood and tissue samples were measured in a gamma counter (Berthold, Wildbad, Germany). Triplicate serial dilutions of the tracer substance were measured simultaneously to adjust for the radioactive decay of ^{111}In . The uptake rates of the paws and the organs were calculated as a percentage of the initially injected radioactivity as well as of the tracer amount present in the circulation.

Pharmacokinetics of radiolabeled MTX

To compare the pharmacokinetics of albumin with the pharmacokinetics of MTX, ~ 0.6 μg of [^3H]MTX (0.74 MBq, dissolved in 50 μl of saline) was injected i.v. into 18 mice with CIA, distributed randomly among six groups. At 10 and 30 min and 1, 3, 24, and 48 h postinjection, three animals of each group were sacrificed. The paws, liver, and kidneys were prepared and weighed, and blood samples were drawn. Radioactivity in the blood and tissue samples was measured as described previously (22). In brief, the tissue and blood samples were solubilized completely using a BTS 450 Tissue Solubilizer (60°C, 8 h). Isopropanol, H_2O_2 , hydrochloric acid, and scintillation cocktail were then added. The samples were measured in a liquid scintillation counter (Tri-Carb 2000; Canberra Packard, Dreieich, Germany), and the uptake of the radiolabeled MTX by the examined tissues and the circulation times were calculated.

Histologic evaluation of the SCID mice implants

To examine albumin uptake by SFs in vivo, 18 SCID mice were distributed randomly among three groups. Sixty days after implantation, 40 μg of free AFLc or either 40 μg of AFLc covalently coupled to albumin (AFLc-HSA) or an equivalent dose of HSA, dissolved in 40 μl of sodium bicarbonate buffer (0.17 M, pH 8.4), were administered to six mice each by i.v. injection into a lateral tail vein. Three mice of each group were sacrificed 3 h and 24 h after injection. The implants were removed and embedded immediately in OCT Tissue-Tek (Diatek, Hallstadt, Germany) embedding medium, and then they were snap frozen and stored at -70°C until further use. The SCID mice implants were cut in 5- μm sections and were examined histologically by fluorescence microscopy (DM RBE; Leica, Heidelberg, Germany). Areas of interest were then analyzed again after staining the sections with H&E.

CLSM of living SFs

To examine albumin uptake and metabolism by SFs in vitro, the cells were cultured (1×10^5 cells/ml) for 24 h and then incubated for 30 min with purpurin-HSA (1 μg purpurin/ml, 200 μg HSA/ml) and acridine orange (1 $\mu\text{g}/\text{ml}$), a marker for late endosomes and lysosomes. After washing with DMEM without phenol red to remove extracellular fluorophores, the living cells were inspected using the Compact Confocal Camera, the European Molecular Biology Laboratory's early prototype of the commercially available LSM 510 (Zeiss, Oberkochen, Germany), equipped with a $\times 63/0.9$ water-dipping objective lens. For excitation of purpurin and acridine

orange, the cells were illuminated at wavelengths of 543 nm and 488 nm, respectively. A set of appropriate filters was used to discriminate the fluorescence of the two dyes and the laser lines. Interline switching of the excitation light provided a virtually simultaneous recording (<10 ms) of the two fluorophores.

Treatment protocol

To evaluate the maximal tolerated dose, we performed toxicity studies with MTX and MTX-HSA in DBA-1 mice by i.p. application of both drugs twice weekly.

To study the effect of MTX and MTX-HSA upon the development of CIA, 199 DBA-1 mice were distributed randomly among five groups. Two weeks after the first immunization with collagen (2 wk before arthritis onset), treatment was started. The animals were treated twice weekly for 4 wk, each mouse receiving eight injections. One group received i.p. injections of saline (group 1, control; $n = 63$). The mice in the four treatment groups were injected i.p. with MTX or MTX-HSA, in two different doses. The animals of groups 2 ($n = 35$) and 3 ($n = 30$) were injected eight times with 7.5 mg and 35 mg of MTX per kilogram of body weight, respectively. Group 4 ($n = 35$) and 5 ($n = 36$) animals were injected eight times with 1.6 mg and 7.5 mg of MTX-HSA per kilogram of body weight, respectively, based on the amount of MTX bound to albumin. After 4 wk of treatment, all mice were sacrificed according to the local animal welfare regulations, which require that mice not be affected by arthritis for longer than 2 wk. During the course of the experiment, twice weekly the mice were inspected for arthritis and side effects of treatment and were weighed. The percentages of mice affected by CIA in each animal group were calculated. Statistical significance was tested using the Fortran-Subroutine Fy test.

Results

Laseroptical visualization of albumin uptake in inflamed paws

Fluorescence-labeled HSA (AFLc-HSA) and free AFLc (control) were administered i.v. to mice with CIA (five mice each), and the inflamed paws were illuminated by laser light 3 h after application. After administration of AFLc, neither healthy nor arthritic paws exhibited fluorescence. Fig. 1 shows white light and fluorescence images taken from a paw of a mouse affected by arthritis after application of AFLc-HSA. In contrast with healthy toes, inflamed toes (Fig. 1, arrows) showed strong fluorescence, indicating that high amounts of albumin accumulate in toes affected by arthritis.

Pharmacokinetics of radiolabeled albumin in comparison with radiolabeled MTX

Radioactive-labeled HSA ($^{111}\text{DTPA}$ -HSA) was injected i.v. into 35 mice with CIA and 21 healthy control mice. Five mice with

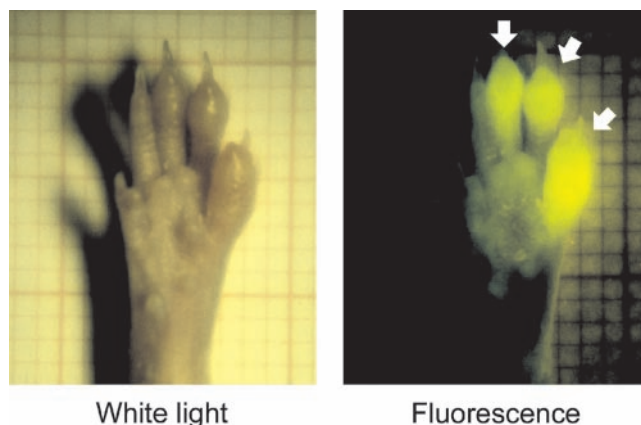
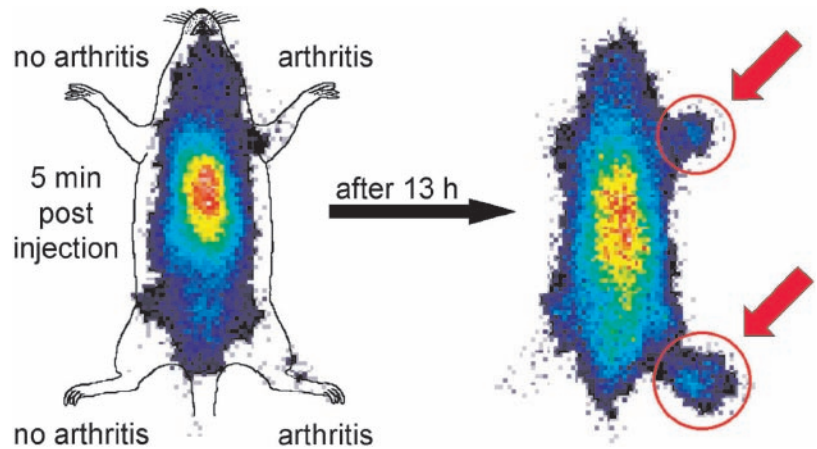


FIGURE 1. Uptake of human serum albumin labeled with aminofluorescein (AFLc-HSA) by inflamed toes of a mouse with CIA as determined by laseroptical imaging. The figure shows white light and fluorescence images taken of an inflamed paw with three arthritic toes (indicated by arrows) 3 h after i.v. injection of AFLc-HSA. Only toes affected by arthritis showed strong fluorescence when illuminated with laser light at 488 nm, demonstrating the high rate of albumin accumulation in inflamed toes.

FIGURE 2. Distribution of radiolabeled HSA ($^{111}\text{In-DTPA-HSA}$) administered i.v. to a mouse with CIA illustrated by scintigraphic imaging. The figure shows scintiscans of a mouse with CIA affecting both right paws 5 min and 13 h after i.v. injection of $^{111}\text{In-DTPA-HSA}$. The color code grading for increasing amounts of radioactivity is blue, green, and yellow followed by red. In contrast with noninflamed paws, arthritic paws (indicated by arrows) accumulated significant amounts of radiolabeled albumin.



CIA and three control mice were sacrificed at seven different time points (10 min and 1, 3, 8, 13, 24, and 48 h) postinjection. Sequential scintiscans were performed to examine the tracer distribution. Another 18 mice with CIA received i.v. injections of radiolabeled MTX (^3H MTX). Three mice each were sacrificed after 10 min, 30 min and 1, 3, 24, and 48 h postinjection. Blood and tissue samples of the mice were collected, the radioactivity in the samples was determined, and the uptake of the tracer into the examined tissues and the circulation times were calculated.

Fig. 2 illustrates scintigraphic images of an arthritic mouse 5 min and 13 h after i.v. injection of radiolabeled albumin. Both right paws were affected by CIA, whereas both left paws showed no visible signs of inflammation. Due to the presence of high tracer amounts in the blood stream, most of the radioactivity was detected over the heart region (red areas on both scintiscans). Five minutes postinjection, none of the paws were visible on the scintiscans. After 13 h, only the inflamed paws (indicated by red arrows), but not the nonarthritic paws, were visible, demonstrating the accumulation of radiolabeled albumin into paws affected by CIA.

The uptake of radiolabeled albumin and radiolabeled MTX by healthy and inflamed hind paws is illustrated in Fig. 3. The maximal accumulation of the albumin tracer in arthritic paws was reached 13 h after application. On average, an individual inflamed hind paw accumulated $3.1 \pm 0.2\%$ of the initially injected radioactivity after 13 h. These values exceeded those of healthy hind paws (maximum uptake $< 0.5\%$) by 6- to 7-fold. In contrast, radiolabeled MTX showed no accumulation in inflamed hind paws. On the contrary, rapidly decreasing amounts of ^3H MTX were found in hind paws affected by arthritis. The highest measurable rate of tracer uptake after administration of radiolabeled MTX was determined 10 min postinjection ($1.3 \pm 0.1\%$), decreasing to $0.5 \pm 0.01\%$ after only 30 min and to $0.15 \pm 0.03\%$ after 48 h, 17-fold less than radiolabeled albumin 48 h after injection. The forepaws showed similar results (data not shown).

The amounts of radiolabeled albumin and radiolabeled MTX present in blood circulation at different time points after injection are shown in Table I. The results demonstrate that significantly more tracer was detectable in the circulation after administration of radiolabeled albumin compared with radiolabeled MTX. After 10 min, $\sim 66\%$ of the albumin tracer could still be found in the circulation, compared with 12% of the MTX tracer, with levels of the albumin tracer decreasing at a lower rate than the levels of radiolabeled MTX. Remarkably, blood levels in mice affected by arthritis at 24 h ($13.5 \pm 1.0\%$) and at 48 h ($6.2 \pm 0.3\%$) after administration of radiolabeled albumin were significantly lower ($p < 0.05$) than the values measured in healthy mice (24 h, $10.9 \pm 1.1\%$; 48 h, $4.6 \pm 0.4\%$).

The uptake rates of radiolabeled albumin and radiolabeled MTX in the liver and kidneys are shown in Tables II and III. No significant differences in albumin tracer uptake by either organ of the arthritic and nonarthritic mice were measurable. After injection of radiolabeled albumin, the detectable radioactivity in the liver decreased from $\sim 10\%$ directly after injection to $\sim 6\%$ after 48 h. In the livers of the mice injected with ^3H MTX, tracer amounts were found to be 3- to 4-fold higher compared with injection of $^{111}\text{In-DTPA-HSA}$, decreasing from $\sim 30\%$ to $\sim 18\%$. Analysis of the kidneys yielded similar results. The albumin tracer uptake rates of the kidneys increased from $\sim 4\%$ 10 min after injection to $\sim 6\%$ at 48 h. After 10 min, 28% of the MTX tracer could be found, decreasing to $\sim 6\%$ after 48 h.

Uptake of albumin in SFs transplanted to SCID mice examined by fluorescence microscopy in vivo

Eighteen SCID mice were implanted s.c. with SFs from a patient with RA, together with normal human articular cartilage. Six mice each received an i.v. injection of fluorescence-labeled albumin (AFLc-HSA), AFLc, or HSA (control animals). Three mice of each group were sacrificed 3 h and 24 h after injection. Implant sections were examined by fluorescence microscopy, then stained

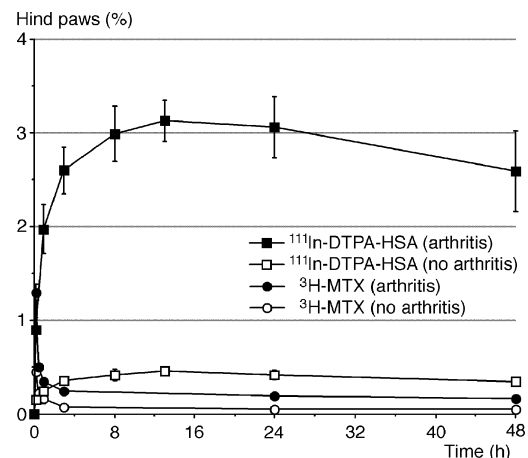


FIGURE 3. Uptake kinetics of radiolabeled HSA ($^{111}\text{In-DTPA-HSA}$) and radiolabeled MTX (^3H MTX) in hind paws of mice with ($n = 3-6$) and without ($n = 3-6$) CIA after i.v. injection. The uptake of the radioactivity in each paw was calculated as percentage of the initially administered tracer amount (mean \pm SD). Significant albumin amounts accumulated in arthritic hind paws, exceeding uptake in noninflamed hind paws by 6- to 7-fold. In contrast, uptake of radiolabeled MTX in arthritic hind paws was found to be significantly less, decreasing rapidly over time.

Table I. Pharmacokinetics of radiolabeled albumin ($^{111}\text{In-DTPA-HSA}$) and radiolabeled MTX ($[^3\text{H}]\text{MTX}$) in blood of mice with and without CIA^a

Time (h)	$^{111}\text{In-DTPA-HSA}$						$[^3\text{H}]\text{MTX}$ Arthritis	
	Without arthritis (n = 3 for each time point)		Arthritis (n = 3 for each time point)		(n = 3 for each time point)			
	Mean	SD	Mean	SD	Mean	SD	Mean	SD
0.17	65.7	1.8	65.0	2.0	12.4	0.9		
0.5	ND	ND	ND	ND	3.1	0.2		
1	53.2	0.7	52.8	1.3	2.2	0.4		
3	40.3	2.0	39.9	2.0	1.9	0.2		
8	25.8	2.1	24.1	1.9	ND	ND		
13	20.0	1.3	18.4	1.1	ND	ND		
24	13.5 ^b	1.0	10.9*	1.1	1.3	0.2		
48	6.2 ^b	0.3	4.6*	0.4	1.0	0.1		

^a The percentages of tracer present in the circulation after i.v. injection of the radiolabeled compounds were calculated based on the initially injected radioactivity.

^b Statistically significant using *t* test; *p* < 0.05. ND, Not done.

with H&E, and evaluated again. In Fig. 4, fluorescence images (*left*) and corresponding H&E images (*right*) of SCID mouse implants are illustrated, showing cartilage and SFs. Fig. 4A shows an implant section of a mouse 24 h after the injection of HSA (control). The fluorescent image demonstrates that in contrast with the cartilage, SFs show a negligible autofluorescence. Fig. 4B illustrates a section of an implant 3 h after injection of AFLc-HSA. SFs are still weakly fluorescent, in contrast with cartilage and sponge fragments, which are highly autofluorescent. Twenty-four hours after injection with AFLc-HSA (Fig. 4, C and D), the cytoplasm of SFs, in contrast with the nuclei, shows strong fluorescence clearly visible in the magnified image (Fig. 4D), demonstrating intensive intracellular uptake of fluorescence-labeled albumin by SFs.

Uptake and metabolism of albumin in SFs examined by CLSM *in vitro*

SFs, isolated from a patient with RA, were cultured and incubated with fluorescence-labeled albumin (purpurin-HSA) and acridine orange, a marker for late endosomes and lysosomes. After washing to remove extracellular fluorescence, cells were inspected by CLSM. As illustrated in Fig. 5, both dyes can be detected in the cytoplasm of the cells, showing a granular fluorescence pattern. The distribution patterns of the fluorescence emitted by the lysosomal marker and fluorescence-labeled albumin in the cells are similar, indicating that albumin is metabolized by SFs in the lysosomal compartment.

Treatment results

Toxicity studies were performed to evaluate the maximum tolerated dose (MTD). When the drugs were applied to five DBA-1

mice per group twice weekly, MTDs of 35 mg/kg body weight for MTX and 7.5 mg/kg for MTX-HSA were calculated.

The difference in the MTD between MTX and MTX-HSA is easily explained by the longer half-life of MTX-HSA, which is ~2 days in comparison with <12 h for MTX, which results in a higher exposure of the mice to MTX-HSA in comparison with MTX when both drugs are given twice weekly. A total of 199 DBA-1 mice was distributed randomly among five groups. One group received saline as a control. The mice in each of the four treatment groups were injected eight times with MTX or MTX-HSA, in two different doses. The animals were weighed and inspected for arthritis and side effects of treatment. The percentages of mice affected by arthritis in each group were calculated. The results of the treatment experiment are illustrated in Fig. 6. Nearly 70% of the control animals developed arthritis during the course of the study. Treatment with 7.5 mg of MTX/kg twice weekly had no significant effect on the onset of CIA, with 57% of the animals affected by arthritis after 4 wk of treatment. In contrast, the equivalent dose of MTX-HSA significantly reduced the development of CIA (28% arthritis incidence, *p* < 0.001). Remarkably, a high MTX dose of 35 mg of MTX/kg twice weekly was required to obtain a result (37% arthritis incidence, *p* = 0.004) compared with 7.5 mg of MTX-HSA/kg. The arthritis incidence in the group treated with 1.6 mg of MTX-HSA/kg (57%) was comparable with that of the 7.5 mg of MTX/kg group. Remarkably, despite the differences in disease incidence between treated and untreated mice, the severity of the disease in the mice that developed arthritis was similar whether they did or did not receive treatment with MTX or MTX-HSA.

Table II. Uptake of radiolabeled albumin ($^{111}\text{In-DTPA-HSA}$) and radiolabeled MTX ($[^3\text{H}]\text{MTX}$) by the liver of mice with and without CIA^a

Time (h)	$^{111}\text{In-DTPA-HSA}$						$[^3\text{H}]\text{MTX}$ Arthritis	
	Without arthritis (n = 3 for each time point)		Arthritis (n = 5 for each time point)		(n = 3 for each time point)			
	Mean	SD	Mean	SD	Mean	SD	Mean	SD
0.17	9.6	0.6	10.7	0.6	25.2	2.0		
0.5	ND	ND	ND	ND	32.2	3.7		
1	8.0	0.7	8.8	0.4	32.2	1.8		
3	6.9	0.4	7.4	0.5	29.4	2.5		
8	6.2	0.5	6.7	0.3	ND	ND		
13	6.0	0.3	6.5	0.2	ND	ND		
24	5.9	0.7	6.3	0.5	19.2	0.7		
48	5.6	0.3	6.0	0.3	17.8	1.7		

^a The percentages of tracer found in the liver after i.v. injection of the radiolabeled compounds were calculated based on the initially injected radioactivity. ND, Not done.

Table III. Uptake of radiolabeled albumin ($^{111}\text{In-DTPA-HSA}$) and radiolabeled MTX ($[^3\text{H}]\text{MTX}$) by the kidneys of mice with and without CIA^a

Time (h)	$^{111}\text{In-DTPA-HSA}$				$[^3\text{H}]\text{MTX}$ Arthritis	
	Without arthritis (<i>n</i> = 3 for each time point)		Arthritis (<i>n</i> = 3 for each time point)		(n = 3 for each time point)	
	Mean	SD	Mean	SD	Mean	SD
0.17	4.0	0.4	3.5	0.4	27.7	3.5
0.5	ND	ND	ND	ND	9.5	2.0
1	4.5	0.3	3.9	0.5	8.3	0.4
3	5.1	0.5	4.5	0.3	8.0	0.7
8	5.8	0.4	5.1	0.4	ND	ND
13	6.3	0.4	5.5	0.4	ND	ND
24	6.7	0.2	6.0	0.5	5.7	0.4
48	6.8	0.2	6.2*	0.5	5.9	0.3

^a The percentages of tracer found in the kidneys after i.v. injection of the radiolabeled compounds were calculated based on the initially injected radioactivity. ND, Not done.

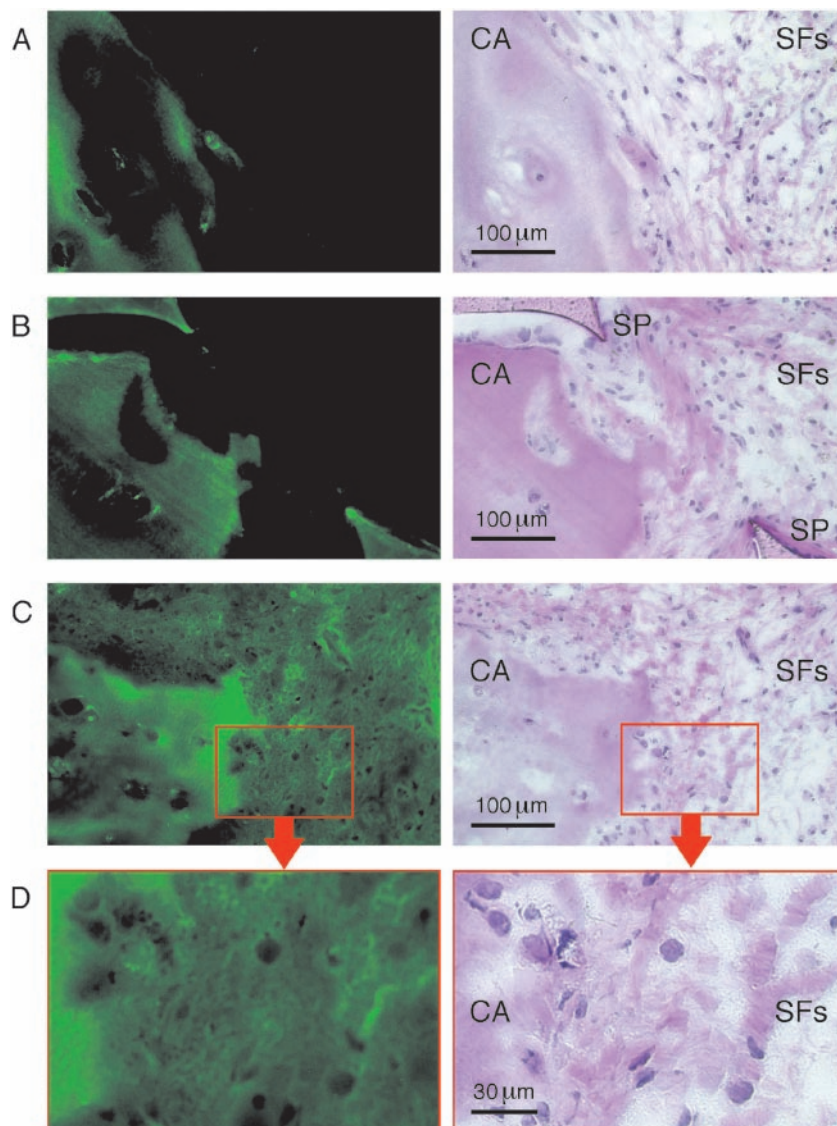
Discussion

The introduction of MTX covalently coupled to HSA (MTX-HSA) as a new therapeutic agent for malignant diseases (21–26) also offers exciting prospects for the future use of MTX-HSA in the treatment inflammatory diseases such as RA. Our preclinical study

demonstrates the favorable properties of albumin as a drug carrier to target inflamed joints of patients with RA.

Several findings indicate that high amounts of albumin accumulate and are metabolized in inflamed joints of RA patients, supporting our concept of albumin-based targeted drug delivery. It is

FIGURE 4. Uptake of fluorescence-labeled albumin by SFs in vivo. *Left*, Fluorescence images of histological sections of SCID mouse implants showing that cartilage (CA) and SFs are presented. *Right*, Same sections stained with H&E are shown. *A*, Section 24 h after i.v. injection of HSA (control). *B*, Section 3 h after i.v. injection of AFLc-HSA. *C*, Section 24 h after i.v. injection of AFLc-HSA. *D*, Magnification of the section shown in *C*. In contrast with cartilage (CA) and sponge fragments (SP), SFs show a negligible autofluorescence. Twenty-four hours after administration of AFLc-HSA, the fluorescence is localized in the cytoplasm of the SFs, demonstrating intracellular albumin uptake by SFs in vivo.



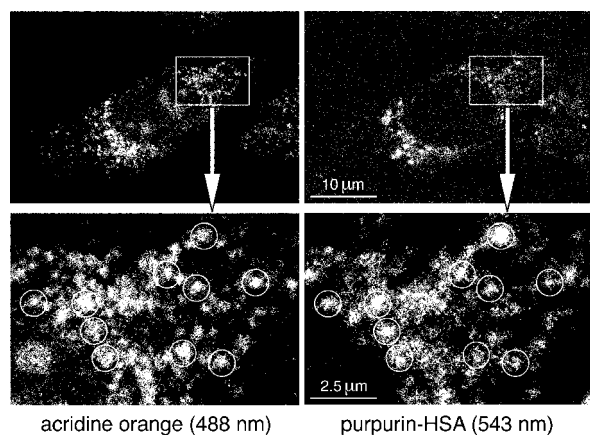


FIGURE 5. Uptake and metabolism of fluorescence-labeled HSA (purpurin-HSA) by cultured human SFs. Confocal images of living SFs 30 min after simultaneous incubation with acridine orange, a marker for late endosomes and lysosomes (excited at 488 nm) and purpurin-HSA (excited at 543 nm) are presented. The fluorescence of both dyes is located in the cytoplasm of the cells, showing similar distribution patterns. The colocalization of the fluorescence demonstrates that albumin is metabolized by SFs in the lysosomal compartment.

well known that the permeability of the blood-joint barrier for albumin is markedly increased in patients with RA (6-fold compared with normal human joints), leading to high albumin concentrations in synovial fluid and inflammatory edema (27). Patients with active RA frequently develop a prominent hypoalbuminemia due to increased albumin turnover, presumably caused by high albumin consumption at sites of inflammation. Wilkinson et al. (28) found that hypoalbuminemia in RA is due neither to a failure of albumin synthesis nor to increased protein loss. Increased vessel permeability also could not be responsible for hypoalbuminemia because the extravascular albumin pool was decreased rather than increased. In contrast, albumin catabolism was increased significantly in RA patients and was related most closely to the activity of the disease (28). Ballantyne et al. (29) confirmed these results. Moreover, Niwa et al. (30) investigated albumin metabolism in 150 patients with RA and systemic lupus erythematosus (SLE). Hypoalbuminemia was found to be more profound in RA than in SLE. In both diseases, albumin catabolism was markedly increased and correlated with the incidence of juxtaarticular erosions in RA. The authors suggested that the increased turnover of albumin in RA and SLE is probably due to high albumin consumption at sites of inflammation and that decreased albumin serum levels in RA are not compensated by increased albumin production (30).

The results of our present study confirmed the findings outlined above. After i.v. application of radiolabeled albumin to mice with and without CIA, a standard mouse model for RA (34–36), we could observe significantly lower tracer levels in blood of arthritic mice compared with healthy mice 24 and 48 h postinjection (Table I). Moreover, we could demonstrate an intensive accumulation of albumin in paws affected by arthritis (Fig. 3). Albumin uptake by inflamed hind paws increased rapidly over time and reached >3% of the amount initially administered into a single arthritic hind paw, exceeding the uptake of healthy hind paws by 6- to 7-fold. The high rate of albumin accumulation in arthritic paws could also be demonstrated by scintigraphy and laseroptical experiments. After injection of radiolabeled albumin, inflamed but not healthy paws were clearly visible on scintiscans (Fig. 2). After application of fluorescence-labeled albumin, inflamed toes were strongly fluorescent, in contrast with noninflamed toes (Fig. 1).

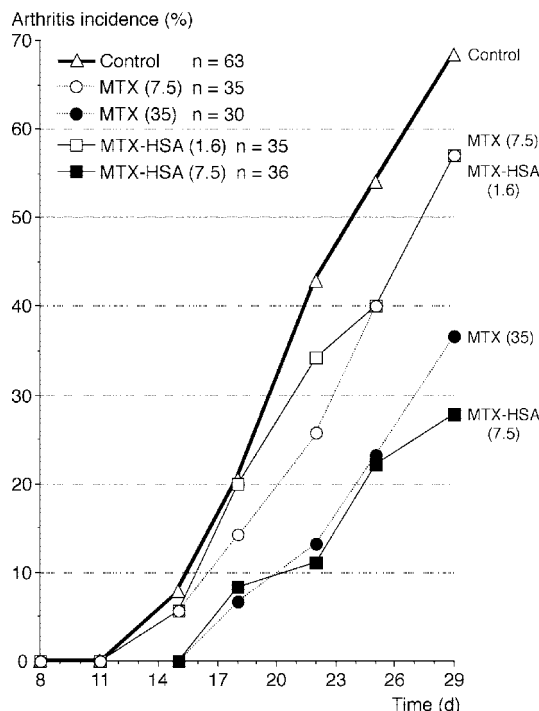


FIGURE 6. Effect of different doses of MTX and MTX-HSA on the development of CIA in mice. The percentages of arthritic mice in each treatment group are presented (arthritis incidence). Treatment was started 2 wk before onset of the disease. The animals were treated for 4 wk and received two i.p. injections weekly. MTX-HSA was significantly more effective in the suppression of the onset of arthritis than were comparable doses of MTX. At least a 5-fold higher dose of MTX was required to achieve the levels of suppression seen with MTX.

In contrast, MTX, the most common drug used in RA, shows unfavorable pharmacokinetic properties with regard to plasma half-life and accumulation in inflamed joints (10–12), leading to unsatisfactory long-term treatment results (6, 7). Therefore, an effective carrier would be desirable, especially to increase exposure times and to provide higher drug concentrations in the synovial tissue and lower drug concentrations in healthy tissue.

The results of this study demonstrate that MTX, in contrast with albumin, is rapidly removed from blood circulation and does not accumulate in inflamed paws. The amounts of MTX detectable in the arthritic paws decreased rapidly from 1.3% after 10 min to 0.5% after 1 h and to 0.15% after 48 h, which corresponds to a 17-fold lower amount than after administration of albumin at the same point of time (Fig. 3). Furthermore, the circulation times of albumin in blood exceeded those of MTX considerably (Table I). These results correspond to previous data in tumor-bearing rats (22). As shown in a phase I clinical trial with cancer patients, the plasma half-life period of HSA and MTX-HSA is ~19 days (26), whereas the half-life period of a low dose of MTX given i.v. to patients with RA is only ~6–8 h (10–12). Because MTX is usually administered once weekly (6, 7), therapeutic MTX concentrations in inflamed joints may only be reached for a short period of time. In contrast, coupling of MTX to albumin has the potential to increase the exposition time and to result in higher MTX concentrations in inflamed joints.

In the liver, three to four times more MTX than albumin was detected (Table II). Due to the renal excretion of MTX, high amounts of the drug could be also measured in the kidneys, especially shortly after i.v. injection. Up to eight times more MTX than albumin could be detected (Table III). As a result, not only MTX

uptake in the target tissue might be increased, but also uptake in the liver and kidneys might be decreased by coupling MTX to albumin.

Because SFs of patients with RA show a high rate of metabolic activation similar to tumor cells (1–5), we considered these cells as potential target cells for albumin-conjugated drugs in inflamed joints. Therefore, we examined albumin uptake by human SFs using the well-established SCID mouse model for RA (37, 38). Fig. 4 demonstrates the intracellular uptake of fluorescence-labeled albumin into SFs derived from patients with RA in vivo. Furthermore, we provide evidence for cellular uptake of fluorescence-labeled albumin in human SFs derived from RA patients in vitro and metabolism of albumin in the lysosomal compartment (Fig. 5). Therefore, it appears most likely that SFs, key players in cartilage and bone destruction within the joints of RA patients (1–5), are affected by treatment with albumin-coupled drugs, especially MTX-HSA.

To complete this preclinical study, we investigated the efficacy of MTX-HSA compared with free MTX in murine CIA. MTX-HSA was significantly more effective in suppression of the onset of arthritis in comparable doses than was MTX (Fig. 6). In comparison with MTX-HSA, at least a 5-fold higher dose of MTX was required to achieve equivalent results.

As is known from the treatment of RA patients, MTX exerts effects only after a treatment period of at least 4 wk. Therefore, the treatment of the mice with MTX or MTX-HSA was started before the onset of arthritis, to evaluate the effect of the treatment on the course of arthritis in the first weeks after onset, which in CIA mice is the most active period of arthritis. Moreover, local animal welfare regulations did not permit the follow up of CIA mice longer than 2 wk after onset of arthritis. This was the reason why the effect of the treatment on the incidence of the disease rather than the reduction of an already established arthritis was measured.

In the present study, we used MTX-coupled HSA to treat DBA-1 mice because murine albumin can be obtained in small quantities only, which makes it difficult to perform in vivo experiments. Because this is a xenologic system, it has the potential to be immunogenic. However, in previous studies we compared the distribution of rat and human albumin in rat (39), which was similar. Moreover, in rats or nude mice, multiple injections of various HSA drug conjugates were well tolerated without signs of allergy or anaphylaxis. Due to the high conservation of albumin in the evolution of mammals and to the similarities between rat and mice as rodents, we hypothesized that interspecies differences between mice and rat in the distribution of human albumin can be neglected. Moreover, because HSA is coupled to the immunosuppressive drug MTX (MTX-HSA), the immunogenicity might be further reduced. This is supported by the finding that the treatment with MTX-HSA did not influence anti-collagen Ab response (data not shown), which should be the case if immunogenicity of HSA would have influenced the immune response to collagen in CIA mice.

MTX-HSA is currently under clinical investigation in several phase II clinical trials for treatment of cancer patients. The initial phase I clinical trial with MTX-HSA showed not only anticancer activity, but the conjugate was also well tolerated for several years without any severe side effects (26). Long-term tolerability is an important aspect, especially in the treatment of RA.

Taking all the data together, albumin appears to be a suitable carrier to target drugs such as MTX not only to neoplastic tissue, but also to inflamed joints of patients with RA, especially to activated SFs. Thus, MTX-albumin might be used to increase the efficacy and reduce toxicity of MTX in the treatment of RA. Moreover, further studies will show whether it will be possible to sub-

stitute weekly doses of MTX with MTX-HSA given i.v. in lower frequencies, such as once monthly, without loss of efficacy.

Acknowledgments

We thank Ulrike Bauder-Wüst for cultivating SFs and Dr. Thomas Haase for assistance during the laseroptical experiments (both from the Department of Medical Physics of the German Cancer Research Center, Heidelberg, Germany). We also gratefully acknowledge the assistance of Nick Salmon of the European Molecular Biology Laboratory (Heidelberg, Germany) for examination of the cells by CLSM and Wibke Ballhorn and Birgit Riepl (University of Regensburg, Germany) for excellent technical assistance in the SCID mouse experiments.

References

- Gay, S., R. E. Gay, and W. J. Koopman. 1993. Molecular and cellular mechanisms of joint destruction in rheumatoid arthritis: two cellular mechanisms explain joint destruction? *Ann. Rheum. Dis.* 52(Suppl. 1):S39.
- Firestein, G. S. 1996. Invasive fibroblast-like synoviocytes in rheumatoid arthritis: passive responders or transformed aggressors? *Arthritis Rheum.* 39:1781.
- Pap, T., U. Müller-Ladner, R. E. Gay, and S. Gay. 2000. Fibroblast biology: role of synovial fibroblasts in the pathogenesis of rheumatoid arthritis. *Arthritis Res.* 2:361.
- Müller-Ladner, U., R. E. Gay, and S. Gay. 1998. Molecular biology of cartilage and bone destruction. *Curr. Opin. Rheumatol.* 10:212.
- Keyszer, G. M., A. H. Heer, J. Kriegsmann, T. Geiler, A. Trabandt, M. Keysser, R. E. Gay, and S. Gay. 1995. Comparative analysis of cathepsin L, cathepsin D, and collagenase messenger RNA expression in synovial tissues of patients with rheumatoid arthritis and osteoarthritis, by in situ hybridization. *Arthritis Rheum.* 38:976.
- Furst, D. E. 1997. The rational use of methotrexate in rheumatoid arthritis and other rheumatic diseases. *Br. J. Rheumatol.* 36:1196.
- O'Dell, J. R. 1997. Methotrexate use in rheumatoid arthritis. *Rheum. Dis. Clin. N. Am.* 23:779.
- Bertino, J. R. 1993. Ode to methotrexate. *J. Clin. Oncol.* 11:5.
- Kaye, S. B. 1998. New antimetabolites in cancer chemotherapy and their clinical impact. *Br. J. Cancer* 78(Suppl. 3):1.
- Herman, R. A., P. Veng Pedersen, J. Hoffman, R. Koehnke, and D. E. Furst. 1989. Pharmacokinetics of low-dose methotrexate in rheumatoid arthritis patients. *J. Pharm. Sci.* 78:165.
- Furst, D. E. 1995. Practical clinical pharmacology and drug interactions of low-dose methotrexate therapy in rheumatoid arthritis. *Br. J. Rheumatol.* 34(Suppl. 2):20.
- Bannwarth, B., F. Pehourcq, T. Schaevebeke, and J. Dehais. 1996. Clinical pharmacokinetics of low-dose pulse methotrexate in rheumatoid arthritis. *Clin. Pharmacokinet.* 30:194.
- Gupta, P. K., J. B. Cannon, and A. K. Tibrewal. 1996. Targeted drug delivery. In *Principles of Antineoplastic Drug Development and Pharmacology*. R. L. Schilsky, G. A. Milano, and M. J. Ratain, eds. Marcel Dekker, New York, p. 587.
- Singh, M., A. J. Ferdous, M. Branham, and G. V. Betergeri. 1996. Trends in drug targeting for cancer treatment. *Drug Deliv.* 3:289.
- Mider, G. B., H. Tesluk, and J. J. Morton. 1948. Effects of Walker carcinoma 256 on food intake, body weight and nitrogen metabolism of growing rats. *Acta Unio Int. Contra Cancrum* 6:409.
- Babson, A. L., and T. Winnick. 1954. Protein transfer in tumor-bearing rats. *Cancer Res.* 14:606.
- Andersson, C., B. M. Iresjö, and K. Lundholm. 1991. Identification of tissue sites for increased albumin degradation in sarcoma-bearing mice. *J. Surg. Res.* 50:156.
- Wunder, A., G. Stehle, H. Sinn, H. H. Schrenk, D. Hoff-Biederbeck, F. Bader, E. A. Friedrich, P. Peschke, W. Maier-Borst, and D. L. Heene. 1997. Enhanced albumin uptake by rat tumors. *Int. J. Oncol.* 11:497.
- Stehle, G., H. Sinn, A. Wunder, H. H. Schrenk, J. C. M. Stewart, G. Hartung, W. Maier-Borst, and D. L. Heene. 1997. Plasma protein (albumin) catabolism by the tumor itself: implications for tumor metabolism and the genesis of cachexia. *Crit. Rev. Oncol. Hematol.* 26:77.
- Jain, R. K. 1988. Determinants of tumor blood flow: a review. *Cancer Res.* 48:2641.
- Stehle, G., H. Sinn, A. Wunder, H. H. Schrenk, S. Schütt, D. L. Heene, and W. Maier-Borst. 1997. The loading rate determines tumor targeting of methotrexate-albumin conjugates in rats. *Anticancer Drugs* 8:677.
- Stehle, G., A. Wunder, H. Sinn, H. H. Schrenk, S. Schütt, E. Frei, G. Hartung, W. Maier-Borst, and D. L. Heene. 1997. Pharmacokinetics of methotrexate-albumin conjugates in tumor bearing rats. *Anticancer Drugs* 8:835.
- Wunder, A., G. Stehle, H. H. Schrenk, G. Hartung, E. Frei, D. L. Heene, W. Maier-Borst, and H. Sinn. 1998. Antitumor activity of methotrexate-albumin conjugates in rats bearing a Walker-256 carcinosarcoma. *Int. J. Cancer* 76:884.
- Stehle, G., A. Wunder, H. H. Schrenk, G. Hartung, D. L. Heene, and H. Sinn. 1999. Methotrexate-albumin conjugate causes tumor growth delay in Dunning R3327 Hi prostate cancer bearing rats. *Anticancer Drugs* 10:405.
- Burger, A. M., G. Hartung, G. Stehle, H. Sinn, and H. H. Fiebig. 2001. Preclinical evaluation of a methotrexate-albumin conjugate (MTX-HSA) in human tumor xenografts in vivo. *Int. J. Cancer* 92:718.

26. Hartung, G., G. Stehle, H. Sinn, A. Wunder, H. H. Schrenk, S. Heeger, M. Kränzle, H. H. Fiebig, E. Frei, L. Edler, et al. 1999. Phase-1 trial of methotrexate-albumin (MTX-HSA) in a weekly intravenous bolus regimen in cancer patients. *Clin. Cancer Res.* 5:753.
27. Levick, J. R. 1981. Permeability of rheumatoid and normal human synovium to specific plasma proteins. *Arthritis Rheum.* 24:1550.
28. Wilkinson, P., R. Jeremy, F. P. Brooks, and J. L. Hollander. 1965. The mechanism of hypoalbuminemia in rheumatoid arthritis. *Ann. Intern. Med.* 63:109.
29. Ballantyne, F. C., A. Fleck, and W. C. Dick. 1971. Albumin metabolism in rheumatoid arthritis. *Ann. Rheum. Dis.* 30:265.
30. Niwa, Y., A. Iio, G. Niwa, T. Sakane, T. Tsunematsu, and T. Kanoh. 1990. Serum albumin metabolism in rheumatic diseases: relationship to corticosteroids and peptic ulcer. *J. Clin. Lab. Immunol.* 31:11.
31. Rinaldi, N., M. Schwarz Eywill, D. Weis, P. Leppelmann Jansen, M. Lukoschek, U. Keilholz, and T. F. Barth. 1997. Increased expression of integrins on fibroblast-like synoviocytes from rheumatoid arthritis in vitro correlates with enhanced binding to extracellular matrix proteins. *Ann. Rheum. Dis.* 56:45.
32. Wooley, P. H. 1988. Collagen-induced arthritis in the mouse. *Methods Enzymol.* 162:361.
33. Judex, M., E. Neumann, M. Fleck, T. Pap, J. Mountz, R. E. Gay, J. Scholmerich, K. Nishioka, S. Gay, and U. Müller-Ladner. 2001. "Inverse wrap": an improved implantation technique for virus-transduced synovial fibroblasts in the SCID mouse model for rheumatoid arthritis (RA). *Mod. Rheumatol.* 11:145.
34. Wooley, P. H. 1991. Animal models of rheumatoid arthritis. *Curr. Opin. Rheumatol.* 3:407.
35. Myers, L. K., E. F. Rosloniec, M. A. Cremer, and A. H. Kang. 1997. Collagen-induced arthritis, an animal model of autoimmunity. *Life Sci.* 61:1861.
36. Joe, B., and R. L. Wilder. 1999. Animal models of rheumatoid arthritis. *Mol. Med. Today* 5:367.
37. Müller-Ladner, U., J. Kriegsmann, B. N. Franklin, S. Matsumoto, T. Geiler, R. E. Gay, and S. Gay. 1996. Synovial fibroblasts of patients with rheumatoid arthritis attach to and invade normal human cartilage when engrafted into SCID mice. *Am. J. Pathol.* 149:1607.
38. Müller-Ladner, U., C. H. Evans, B. N. Franklin, C. R. Roberts, R. E. Gay, P. D. Robbins, and S. Gay. 1999. Gene transfer of cytokine inhibitors into human synovial fibroblasts in the SCID mouse model. *Arthritis Rheum.* 42:490.
39. Stehle, G., A. Wunder, H. H. Schrenk, G. Hartung, D. L. Heene, and H. Sinn. 1999. Albumin-based drug carriers: comparison between serum albumins of different species on pharmacokinetics and tumor uptake of the conjugate. *Anticancer Drugs* 10:785.